Vol 15 No 3, March 2006
1009-1963/2006/15(03)/0568-07

Chinese Physics

© 2006 Chin. Phys. Soc.
and IOP Publishing Ltd

Successive particle acceleration by use of two tightly focused ultra-short intense laser pulses*

Chen Min(陈 民), Sheng Zheng-Ming(盛政明), and Zhang Jie(张 杰)†

Laboratory of Optical Physics, Institute of Physics, Chinese Academy of Sciences, Beijing 100080, *China*

(Received 21 May 2005; revised manuscript received 30 June 2005)

We suggest a scheme of electron acceleration by use of two tightly focused ultra-short intense laser pulses at a 100TW level. Electrons obtain a preliminary acceleration with a small angular spread by the longitudinal ponderomotive force of the first pulse. They are then injected and further accelerated to hundreds of MeV by the second laser pulse.

Keywords: laser acceleration, particle acceleration, plasmas
PACC: 5240D, 5275D, 4260, 2910

1. Introduction

The rapid advances in laser technology[1,2] make the laser acceleration possible. Many acceleration schemes have been proposed. Such as the plasma beatwave accelerator (PBWA),[3,4] plasma wakefield accelerator (PWFA),[5,6] the laser wakefield accelerator (LWFA),[7] the betatron-resonance acceleration in the self-focusing channel of laser pulses,[8] and the stochastic heating by counter-directionally propagating laser pulses in plasmas.[9] In all of these processes, the particles are accelerated in plasmas. Electrons can also been accelerated to high energies by laser fields in vacuum.[10−17] It is well known that planar electromagnetic waves do not serve the function of electron acceleration in vacuum because of the symmetrical motion. For electrons to obtain a significant energy gain, this symmetrical motion must be broken. Based on this idea, a lot of proposals have been proposed. One of such proposals is to use a tightly focused laser pulse, where the forward acceleration by the longitudinal ponderomotive force at the pulse front edge is larger than the deceleration at the pulse trailing edge.[18−20] In another proposal, the electrons are injected from the brim of the laser beam.[13,15−17]

However, it is found that electron acceleration in the first proposal mentioned above is not very efficient, i.e. the energy gain is small even though the accelerated electrons have a small angular spread. Electrons accelerated in the second scheme can obtain more energy gain. However in that scheme Ho *et al* have adopted a laser field of infinite pulse duration, which is unreasonable for today's technology.

In this paper, we study the second injection scheme with an ultra-short pulse whose field is a second-order field both for the transverse and longitudinal small parameters ε and σ (defined later) instead of infinite pulse or the usually used lowest-order Hermite–Gaussian (0,0) mode with analytical expressions in the paraxial approximation. Then we combine it with the first scheme to accelerate electrons to hundreds of MeV using two 100TW laser pulses.

2. The acceleration model and laser field

In our proposal, a test electron is accelerated by two successive laser pulses. Figure 1 shows the interaction geometry in the $x-z$ plane. A test electron initially at rest is located at the focus of the first laser pulse. The focus of the second laser pulse is at (z_0, x_0), and the angle between the two laser beams is

*Project supported by the National Natural Science Foundation of China (Grant Nos 10335020, 10105014 and 10390160), the National High Technology Inertial Confinement Fusion Foundation of China, and the National Key Basic Research Special Foundation of China (Grant No G1999075200).

†Corresponding author. E-mail: jzhang@aphy.iphy.ac.cn

θ_i. Firstly, the electron is accelerated by the first laser pulse under the action of the longitudinal ponderomotive force. Then it is injected to the second laser pulse at a velocity approaching the light speed in vacuum.

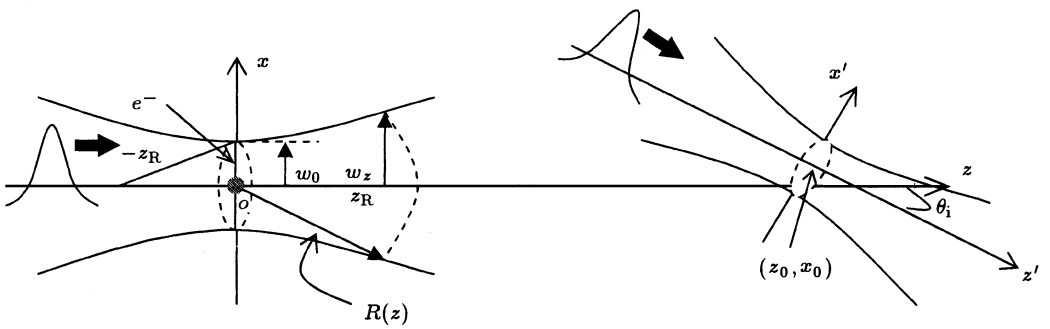


Fig.1. The interaction geometry between the laser pulse and the test electron. The electron is initially located at the focus of the first laser pulse $(0, 0)$.

A monochromatic laser field can be described as follows:[14,21−23]

$$E_x = ES_0 + E\varepsilon^2\left[\xi^2 S_2 - \frac{\rho^4 S_3}{4}\right], \tag{1}$$

$$E_y = E\xi\nu\varepsilon^2 S_2, \tag{2}$$

$$E_z = E\xi\varepsilon C_1, \tag{3}$$

$$B_x = 0, \tag{4}$$

$$B_y = ES_0 + E\varepsilon^2\left[\frac{\rho^2 S_2}{2} - \frac{\rho^4 S_3}{4}\right], \tag{5}$$

$$B_z = E\nu\varepsilon C_1, \tag{6}$$

where $\xi = x/w_0$, $\nu = y/w_0$, $r^2 = x^2 + y^2$, $\rho = r/w_0$, and $E = E_0\dfrac{w_0}{w}\exp\left[-\dfrac{r^2}{w^2}\right]$ for a beam radius at the focus w_0, the radius away from the focus $w(z) = w_0\sqrt{1 + (z/z_R)^2}$, the Rayleigh length $z_R = kw_0^2/2$, $k = 2\pi/\lambda$, and the diffraction angle $\varepsilon = w_0/z_R$. Also there are the following expressions:

$$S_n = \left(\frac{w_0}{w}\right)^n \sin(\psi + n\psi_G);$$

$$C_n = \left(\frac{w_0}{w}\right)^n \cos(\psi + n\psi_G), \quad n = 0, 1, 2, ...,$$

where $\psi = \psi_0 + \psi_P - \psi_R + \psi_G$, ψ_0 is a constant phase, $\psi_P = \eta = \omega t - kz$ is the plane wave phase, $\psi_G = \tan^{-1}(z/z_R)$ is the Guoy phase associated with the fact that a Gaussian beam undergoes a total phase change of π as z changes from $-\infty$ to $+\infty$, $\psi_R = kr^2/(2R)$ is the phase associated with the curvature of the wave fronts, $R(z) = z + z_R^2/z$ is the radius of curvature of a wave front intersecting the beam axis at the coordinate z. The fields given above satisfy the Maxwell's equations in vacuum up to the order of ε^2.

For a laser pulse with finite duration, we must add the temporally modified terms to the above field by using the Fourier transform. Here we derive the field expressions with higher order corrections using the method Quesnel and Mora proposed[21] and take the transverse electric field as an example. Suppose the laser pulse to be polarized in the x direction and have a Gaussian profile with beam waist at focus and a Gaussian profile temporal envelop $f(t)$. The central frequency of the pulse is ω_0. Then the electric field in the x direction at the focus can be described as: $E_x(x, y, z = 0, t) = E_0(x, y)f(t)\exp(-i\omega_0 t)$, and $E_0(x, y) = E_0\exp[-(x^2 + y^2)/w_0^2]$. The temporal Fourier transform of this expression yields $E_x(x, y, z = 0, \omega) = E_0(x, y)\tilde{f}(\omega - \omega_0)$, where $\tilde{f}(\omega)$ is the Fourier transform of $f(t)$. Defining $\tilde{E}_x(p, q, \omega) = \tilde{f}(\omega - \omega_0)\dfrac{1}{\lambda^2}\iint E_0(x, y)\mathrm{e}^{-\mathrm{i}k(px+qy)}\mathrm{d}x\mathrm{d}y$, where $k = \omega/c$ and $\lambda = 2\pi c/\omega$, it is then easy to show that E_x can be computed at any point in space using

$$E_x(x, y, z, t) = \int \mathrm{d}\omega \mathrm{e}^{-\mathrm{i}\omega t}\iint \mathrm{d}p\mathrm{d}q\tilde{E}_x(p, q, \omega) \times \mathrm{e}^{\mathrm{i}k(px+qy+mz)}. \tag{7}$$

Here $m = \begin{cases} \left(1 - p^2 - q^2\right)^{1/2}, & \text{if} \quad p^2 + q^2 \le 1 \\ \mathrm{i}\left(p^2 + q^2 - 1\right)^{1/2}, & \text{if} \quad p^2 + q^2 > 1 \end{cases}$

Defining

$$\mathrm{e}^{\mathrm{i}kz}\breve{E}(x, y, z, \omega)\tilde{f}(\omega - \omega_0) = \iint \mathrm{d}p\mathrm{d}q\tilde{E}_x(p, q, \omega)\mathrm{e}^{\mathrm{i}k(px+qy+mz)},$$

we obtain

$$E_x(x, y, z, t) = \int \mathrm{d}\omega \mathrm{e}^{-\mathrm{i}\omega t}\mathrm{e}^{\mathrm{i}kz}\breve{E}(x, y, z, \omega) \times \tilde{f}(\omega - \omega_0).$$

The important property of $\breve{E}$ here is that it is a slowly varying function of ω with respect to the $\mathrm{e}^{-\mathrm{i}\omega t}$ terms. Expanding the field to $\breve{E}(x, y, z, \omega)$ with the parameter ω by using Taylor expansion, one obtains

$$
\begin{aligned}
E_x(x,y,z,t) =& \breve{E}(x,y,z,\omega_0)\int \mathrm{d}\omega \mathrm{e}^{-\mathrm{i}\omega(t-z/c)}\tilde{f}(\omega-\omega_0)+\frac{\partial \breve{E}}{\partial\omega}(x,y,z,\omega_0)\int \mathrm{d}\omega \mathrm{e}^{-\mathrm{i}\omega(t-z/c)} \\
&\times(\omega-\omega_0)\tilde{f}(\omega-\omega_0)+\frac{\partial^2 \breve{E}}{\partial\omega^2}(x,y,z,\omega_0)\int \mathrm{d}\omega \mathrm{e}^{-\mathrm{i}\omega(t-z/c)}(\omega-\omega_0)^2\tilde{f}(\omega-\omega_0)+\cdots \\
=& \breve{E}(x,y,z,\omega_0)\mathrm{e}^{\mathrm{i}k_0(z-ct)}f(t-z/c)+\frac{\partial \breve{E}}{\partial\omega}(x,y,z,\omega_0)\mathrm{e}^{\mathrm{i}k_0(z-ct)}if'(t-z/c) \\
&-\frac{\partial^2 \breve{E}}{\partial\omega^2}(x,y,z,\omega_0)\mathrm{e}^{\mathrm{i}k_0(z-ct)}f''(t-z/c)\cdots . \qquad (8)
\end{aligned}
$$

In our simulation, $f(t)=\mathrm{e}^{-t^2/\eta^2}$, we define the longitudinal small parameter $\sigma=2\pi/\omega_0\eta$. The successive derivatives of f are proportional to the successive powers of σ, so that we can obtain the infinite expansions. In our computation, we transform Salamin's second-order field[14] to $\breve{E}(x,y,z,\omega_0)$ and then expand the temporal factor to the second-order. As a result, our last field is an second-order field both for the transverse and longitudinal small parameters ε and σ, respectively. All the other components of the field are treated similarly.

As usual, we discuss the dynamics of a test electron with mass m and charge $-e$ by numerically solving the dynamical equation

$$
\frac{\mathrm{d}\boldsymbol{r}}{\mathrm{d}t}=\frac{\boldsymbol{p}}{\gamma},\ \frac{\mathrm{d}\boldsymbol{p}}{\mathrm{d}t}=-2\pi[\boldsymbol{E}+\boldsymbol{\beta}\times\boldsymbol{B}], \qquad (9)
$$

where the Lorentz factor $\gamma=\left(1-\boldsymbol{\beta}^2\right)^{-1/2}$, $\boldsymbol{\beta}$ is the electron's velocity normalized by the speed of light c in vacuum, $\boldsymbol{p}=\gamma\boldsymbol{\beta}$ is the momentum normalized by mc, the spatial coordinates $\boldsymbol{r}$ and the time t are normalized by wavelength λ and laser period T, respectively, the electronic field $\boldsymbol{E}$ and magnetic field $\boldsymbol{B}$ are both normalized by $mc\omega/e$. We use the fourth-order Runge–Kutta method with time-step changing to keep the simulations in a high accuracy. The minimal time step is $0.001T$, which is sufficient for the fields considered in this paper. In our simulations, the parameters for both laser fields are fixed. We take focus radius w_0=7μm and 10μm, respectively, for the first and second lasers, the laser wavelength is 1μm, the peak intensity is $1.375\times10^{20}\mathrm{W/cm}^2$, corresponding to a laser power around 100TW for both pulses. By using the well-known formula $I_0\lambda^2\approx1.375\times10^{18}a^2$, the normalized field amplitude $a=eE_0/mc\omega_0=10$. For both of the two acceleration processes, a typical simulation runs up to a time period of about $50000T_0$. This is long enough to obtain the electron's final energy and trajectory.

3. Different acceleration processes

3.1. Ponderomotive acceleration

As has been mentioned, an electron initially at rest, located near the focus on the axis, can be accelerated by a laser pulse. Since it has been studied extensively before,[18−20] we just describe it briefly here. Figure 2 shows one of our simulations, where, the laser pulse duration is $40T_0$ measured when the laser intensity decreases to $1/e^2$ of the peak value. We find the final energy of the electron is $23.6mc^2$ and the transverse deviation is only $0.17\lambda_0$ when it moves a longitudinal distance of $50000\lambda_0$. The corresponding emission angle is $(9.75\times10^{-4})^\circ$. This is an electron source suitable for injection into the second pulse for being further accelerated. If the pulse duration changes, the final energy gain also changes, as shown in Fig.3, where it is shown that the maximum

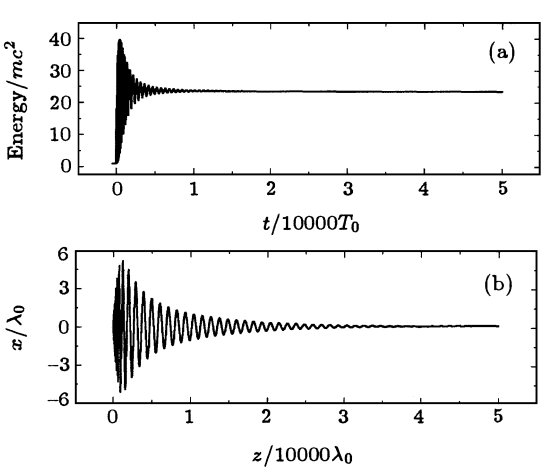


Fig.2. (a) The electron energy changes with time; (b) the electron trajectory.

energy gain is below $24mc^2$, which is small compared with the energy gains in other laser acceleration proposals.

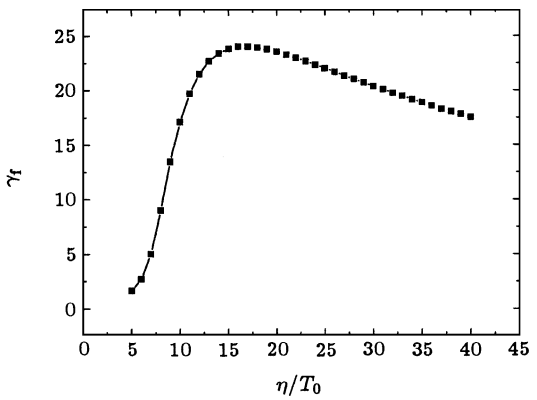


Fig.3. The electron final energy versus laser pulse duration for the first acceleration project. The laser's parameters are E_0=10.0 $mc\omega_0/e$, $w_0 = 7.0\lambda_0$. The electron is initially at rest and located at the laser pulse's focus (0, 0).

3.2. Laser acceleration for oblique injection of electrons

When a test electron is injected obliquely into a high-amplitude laser field properly, it can gain significant energy.[13–17] However, in most of these calculations, the used pulse durations are infinite. Here we conduct some new calculations with finite pulse durations taken into account. Consider that an electron with initial momentum p_0, initially located at (z_0, x_0), is injected into an laser field focused at (0,0). Figure 4 is a typical case, in which the laser pulse has a focus radius $w_0 = 10\lambda_0$, a peak amplitude $a = E_0e/(mc\omega_0) = 10.0$, a pulse duration 2η=$40T_0$, the initial phase $\psi_0 = 0.75\pi$, and the initial pulse centre at $z_0 = -3212\lambda_0$. The electron is injected at the point of $(x_0, y_0, z_0) = (-241, 0, -3200)$ at an injection angle $\theta_i = 4.45°$ with injection momentum $p_0 = 20mc$. After interaction, the final energy is $304.9mc^2$, corresponding to an energy gain of $284.9mc^2$.

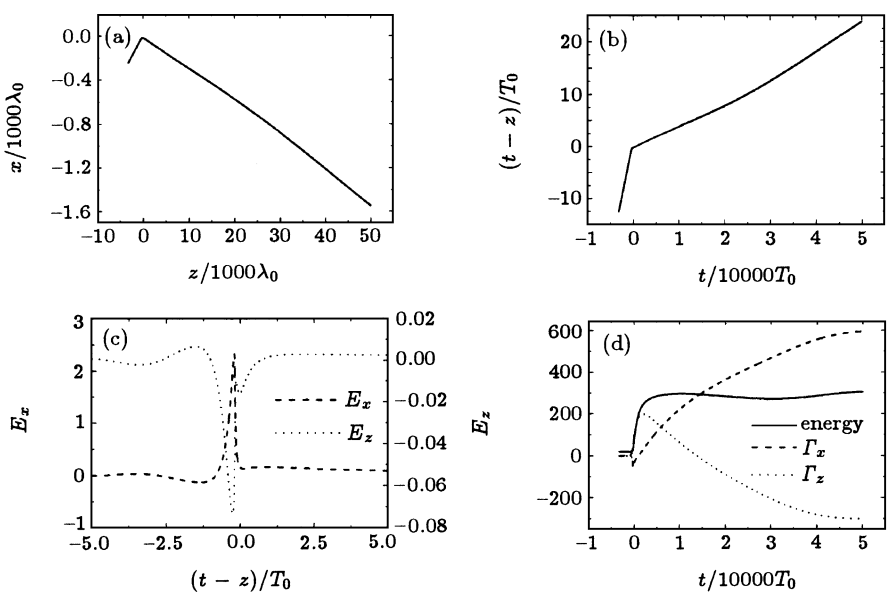


Fig.4. (a) The electron trajectory; (b) the relative phase; (c) the transverse electric field the electron feels (dashed line), and the longitudinal field (dotted line); in quite a long time both of the fields the electron feels are unipolar; (d) the work done by transverse (dashed line) and longitudinal (dotted line) fields and for the electron's total energy (solid line).

It is known that both the longitudinal and the transverse field components in focused laser pulses can contribute to the electron acceleration. Some earlier studies suggested that the longitudinal field played a dominant role in the acceleration, while some others suggested that the ponderomotive force (or the transverse field) played a dominant role. To clarify the acceleration mechanism, one can use the following relationship[9]:

$$\begin{aligned} \mathrm{d}\gamma/\mathrm{d}t =& -2\pi(\beta_x E_x + \beta_y E_y + \beta_z E_z) \\ \equiv& \mathrm{d}\gamma_\perp/\mathrm{d}t + \mathrm{d}\gamma_z/\mathrm{d}t, \end{aligned} \tag{10}$$

which is obtained from the equation of motion. Here $\gamma_\perp$ and γ_z represent the energy gains from the transverse and longitudinal fields, respectively. Figure 4(d) shows that at the beginning the energy gain for tra-

jectory is dominantly due to γ_z, i.e. the longitudinal field. Later on, γ_z decreases slowly while $\gamma_\perp$ increases slowly in quite a long distance until the electron is far from the focus, typically $5000\lambda_0$. However, the total energy remains almost constant since the electron has moved about $1000\lambda_0$. The energy gains from the transverse and longitudinal fields cancel each other out as electrons move far from the laser focus.[24] Figures 4(b), 4(c) and 4(d) show that the electron remains in phase with the laser pulse for a long time because of its high speed and the field structure. One finds that both the transverse and longitudinal fields contribute to the energy gain of the electron.

To study the effect of the finite pulse duration on the energy gain, we plot the energy gain against the pulse duration in Fig.5. It shows that the energy gain exponentially increases with the pulse duration in a way approximately as $\Delta E/mc^2 = ae^{-\eta/b} + \Delta E_{\max}$. For the parameters we used for the laser pulse and the test electron, we have $a = -171.9$, $b = 10.1$ and $\Delta E_{\max} = 95.6$. This shows that a long pulse is unnecessary since it is not much beneficial to the acceleration. However, a very short duration always results in a small energy gain. This is because the large laser intensity gradient in the longitudinal direction can lead to an large deflection of the electron. To be reasonable, we adopt $\eta = 20$, i.e. pulse duration is $40T_0$, in the following section.

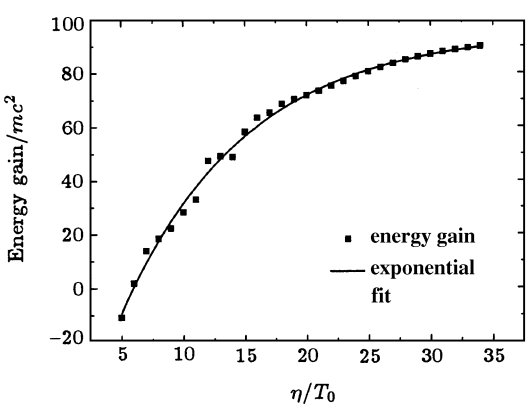


Fig.5. Electron energy gain vs the laser pulse duration. The solid line is an exponential fit. Here, the electron is injected at $(z_0, x_0) = (-3200, -241.5)$ with initial momentum $p_0 = 20.0$ at an injection angle $\theta_i = 4.0°$, the laser initial phase being $\psi_0 = 0.75\pi$.

Figure 6(a) shows the final energy of the test electron as a function of the initial phase of the pulse. In a wide range of the initial phase, the electron can gain a large energy. This is advantageous to the acceleration. At the same time, if one changes the relative time delay between the pulse and the electron to arrive

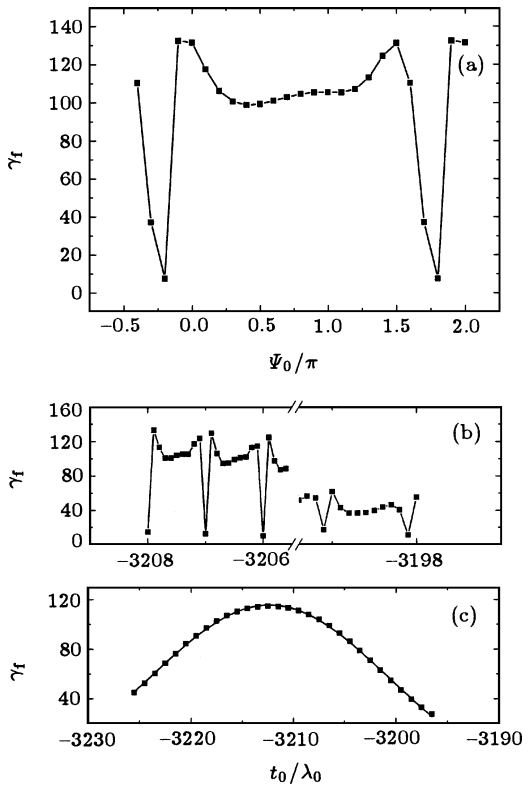


Fig.6. (a) The electron's final energy versus the laser pulse initial phase. For all of the dots, the electron's initial momentum is $20mc$. Except for laser duration $\eta = 20.0$, all other parameters are the same as those in Fig.5. (b) The fine structure for a small change of t_0. (c) The global tendency of electron's final energy vs the relative delay time t_0 of laser pulse. The solid line is its Gaussian fit curve.

at the laser focus by changing the pulse's initial centre t_0, it is equivalent to changing the initial phase. Figure 6(b) shows the final energy as a function of the time delay. It is found that there are periodic drops in the energy gain in a cycle of every 2π in between. The energy gain is relatively stable at certain levels. Figure 6(c) shows the stable energy gain over a large range of the time delay t_0. It appears that this energy gain can be fitted by a Gaussian function:

$$\gamma_f = \gamma_0 + \frac{A}{\sqrt{2\pi}t_1}\exp\left(-\frac{1}{2}\left(\frac{t_0 - t_{\rm m}}{t_1}\right)^2\right), \qquad (11)$$

where $\gamma_0 = -34.8$, $t_{\rm m} = -3212.3$, $t_1 = 11.7$, $A = 4424.1$. The maximum energy gain corresponds to $t_0 = t_{\rm m} = -3212.3 \approx -3211.8 = -t_{\rm u}$, $t_{\rm u}$ is the flight time for electron to reach the focus plane when there is no laser pulse. This means when the electron is synchronous with the laser pulse it will obtain a largest energy gain. The time delay width for energy gain $> 50mc^2$ is about $20T_0$. With laser pulse parameters,

and the injection point and angle all fixed, we can also change the initial injection momentum. There exists a high flat top with $49 \leq p_0 \leq 58$ in Fig.7. However, this injection momentum is still too large for our successive acceleration purpose since electrons accelerated by the first process usually have energies less than $24mc^2$, as shown in Fig.3.

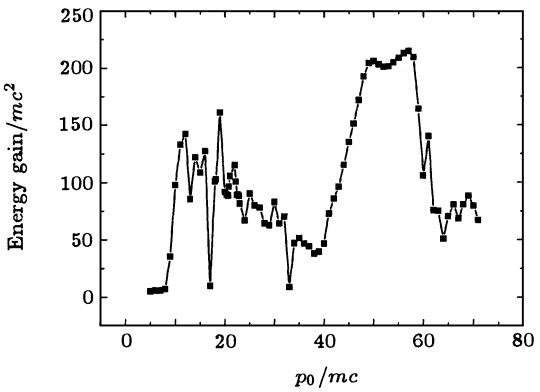


Fig.7. Energy gain versus initial injection momentum. Here $\eta = 20.0$, all other parameters are the same as those in Fig.4.

For this purpose, one needs to optimize other parameters. The injection angle is another important variable. Figure 8 shows the electron energy gain as a function of the injection angle for a given injection momentum p_0=20. Different injection angles give different interaction points between the laser pulse and electron. Figure 8 shows that when the injection angle equals 4.45°, the electron can obtain energy up to about 120MeV that is treble larger than that in the case of smaller injection angle.

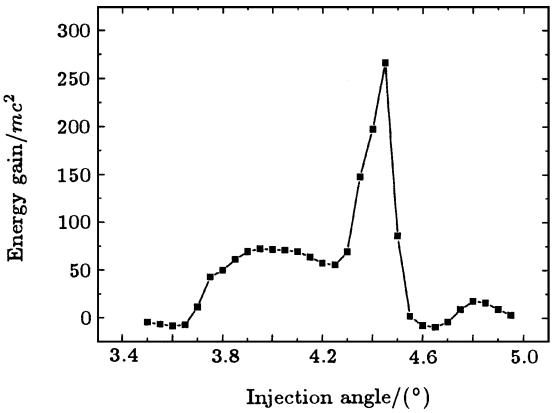


Fig.8. The electron energy gain versus injection angle. Here $p_0 = 20.0$, all the other parameters are the same as in Fig.7.

3.3. Successive acceleration by two laser pulses

Now we consider successive acceleration of electrons by two laser pulses. We combine our simulations of the two different acceleration processes. Figure 1 shows the interaction geometry, where the second laser pulse is focused at (z_0, x_0), which is far from that of the first pulse. Since the electron accelerated by the first pulse moves almost along its propagation axis, the injection angle to the second laser pulse can be changed by setting the second laser's crossing angle. By adjusting the relative delay between the two laser pulses to about Z_0/c, the electron can interact with the second laser at the right time. To change the injection momentum of the electron into the second laser pulse, one can change the first laser pulse's duration, as shown in Fig.3. In this way, one can control the three critical parameters θ_i, t_0, p_0 in experiments.

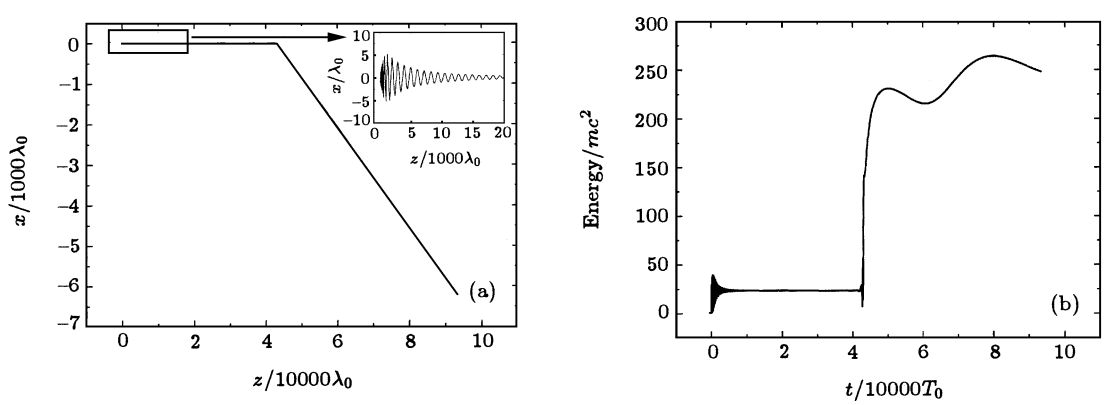


Fig.9. Two laser pulses accelerate an electron to 127MeV. The first laser pulse parameters are $a = 10.0$, $\eta = 20.0$, and $w_0 = 7.0$, the second laser pulse parameters are $a = 10.0$, $\eta = 20.0$, and $w_0 = 10.0$. The angle between the two lasers is $\theta = 4.65°$.

In an example of simulation showing the successive acceleration, we accelerate an electron initially at rest to 120MeV. Figure 9(a) shows the electron trajectory in the $x - z$ plane. Figure 9(b) shows its energy as a function of time. It is certainly possible to optimize the relevant parameters so that the energy gain can be made even larger.

4. Summary

By using test particle simulations, we have studied the ponderomotive acceleration for electrons initially at rest and laser field acceleration for injected electrons by tightly focused laser pulses. For the first case, the accelerated electrons have not very high energy but have very small angular spread. For the second case, electrons can gain high energy. Energy gains are calculated for different pulse parameters and injection electron parameters. For an electron initially at rest, we propose a scheme of successive acceleration by use of two laser pulses, where the first pulse can provide a primary acceleration for the electron, which is then injected into the second laser pulse for further being accelerated. An example of simulation is given, in which electrons can be accelerated to 120 MeV by two 100TW laser pulses.

References

[1] Strickland D and Mourou G 1985 *Opt. Commun.* **264** 219

[2] Maine P, Strickland D, Pessot M and Mourou G 1988 *IEEE J. Quantum Electron.* **QE-24** 298

[3] Tajima T and Dawson J M 1979 *Phys. Rev. Lett.* **43** 267

[4] Kitagawa Y, Matsumoto Y, Minamihata Y, Sawai K, Matsuo K, Mima K, Nishihara K, Azechi H, Tanaka K A, Takabe H and Nakai S 1992 *Phys. Rev. Lett.* **68** 48

[5] Rosenzweig J B, Cline D B, Cole B, Figueroa H, Gai W, Konecny R, Norem J, Schoessow P and Simpson J 1988 *Phys. Rev. Lett.* **61** 98

[6] Rosenzweig J B, Schoessow P, Cole B, Gai W, Konecny R, Norem J and Simpson J 1989 *Phys. Rev.* A **39** 1586

[7] Chiou T C, Katsouleas T, Decker C, Mori W B, Wurtele J S, Shvets G and Su J J 1995 *Phys. Plasmas* **2** 310

[8] Pukhov A, Sheng Z M and Meyer-ter-Vehn J 1999 *Phys. Plasmas* **6** 2847

[9] Sheng Z M, Mima K, Sentoku K, Jovanovi M S, Taguchi T, Zhang J and Meyer-ter-Vehn J 2002 *Phys. Rev. Lett.* **88** 055004
Sheng Z M, Mima K, Zhang J and Meyer-ter-Vehn J 2004 *Phys. Rev.* E **69** 016407

[10] Scully M O and Zubairy M S 1991 *Phys. Rev.* A **44** 2656

[11] Hartemann F V, Fochs S N, Le Sage G P, Luhamann N C, Woodworth J G, Perry M D, Chen Y J and Kerman A K 1995 *Phys. Rev.* E **51** 4833

[12] Malka G, Lefebvre E and Miquel J L 1997 *Phys. Rev. Lett.* **78** 3314

[13] Wang J X, Ho Y K, Feng L, Kong Q, Wang P X, Yuan Z S and Scheid W 1999 *Phys. Rev.* E **60** 7473

[14] Salamin Y I and Keitel C H 2002 *Phys. Rev. Lett.* **88** 095005
Salamin Y I, Mocken G R and Keitel C H 2003 *Phys. Rev.* E **67** 016501

[15] Pang J, Ho Y K, Cao N, Shao L, Xie Y J, Chen Z and Zhang S Y 2003 *Appl. Phys.* B **76** 617

[16] Wang J X, Ho Y K, Kong Q, Zhu L J, Feng L, Scheid S and Hora H 1998 *Phys. Rev.* E **58** 6575
Kong Q, Ho Y K, Wang J X, Wang P X, Feng L and Yuan Z S 2000 *Phys. Rev.* E **61** 1981

[17] Ho Y K, Wang J X, Feng L, Scheid W and Hora H 1996 *Phys. Lett.* A **220** 189

[18] Stupakov G V and Zolotorev M S 2001 *Phys. Rev. Lett.* **86** 5274

[19] He F, Yu W, Lu P X, Xu H, Qian L J, Shen B F, Yuan X, Li R X and Xu Z Z 2003 *Phys. Rev.* E **68** 046407

[20] He F, Yu W, Lu P X, Yuan X and Liu J R 2004 *Acta Phys. Sin.* **53** 165

[21] Quesnel B and Mora P 1998 *Phys. Rev.* E **58** 3719

[22] Davis L W 1979 *Phys. Rev.* A **19** 1177

[23] Scully M O and Zubairy M S 1991 *Phys. Rev.* A **44** 2656

[24] Chen M, Sheng Z M and Zhang J 2005 *Chin. Phys.* **14** 1407